

A. ZUCCHINI



IT03\$0054

**A THERMO-MECHANICAL BENCHMARK CALCULATION
OF AN HEXAGONAL CAN IN THE BTI
ACCIDENT WITH ABAQUS CODE**



COMITATO NAZIONALE PER LA RICERCA E PER LO SVILUPPO
DELL'ENERGIA NUCLEARE E DELLE ENERGIE ALTERNATIVE

A THERMO-MECHANICAL BENCHMARK CALCULATION OF AN HEXAGONAL CAN IN THE BTI ACCIDENT WITH ABAQUS CODE

A. ZUCCHINI

ENEA - Dipartimento Tecnologie Intersettoriali di Base,
Centro Ricerche Energia "Ezio Clementel", Bologna

RT/TIB/88/16

Testo pervenuto nel luglio 1988
Progetto Enea: Sistema nocciolo e sicurezza (VW)

This work has been performed within the framework of the international agreement AGT4 (WP3)

I contenuti tecnico-scientifici dei rapporti tecnici dell'Enea
rispecchiano l'opinione degli autori e non necessariamente quella dell'ente.

Summary :

The thermo-mechanical behaviour of an hexagonal can in a benchmark problem (simulating the conditions of a BTI accident in a fuel assembly) is examined by means of the ABAQUS code : the effects of the geometric nonlinearity are shown and the results are compared with those of a previous analysis performed with the INCA code.

Riassunto :

Il comportamento termo-meccanico di una scatola esagonale in un caso benchmark (simulante le condizioni di un incidente di BTI in un elemento di combustibile) e' studiato con il codice ABAQUS : vengono evidenziati gli effetti della non linearita' geometrica e i risultati sono confrontati con quelli di una precedente analisi eseguita con il codice INCA.

CONTENTS

1) Introduction

2) Benchmark

3) Calculations

4) Results

5) Conclusions

Figures

Appendix

References

1) Introduction

The safety analysis for LMFBR requires the knowledge of the mechanical behaviour of the hexagonal can of a fuel subassembly undergoing a BTI accident (instantaneous total plugging).

The problem is quite complicated because beside the plastic deformation due to thermal and pressure loads we have to face the partial melting of the can itself.

In the frame of these studies a mechanical benchmark problem has been created, starting from realistic SPX1 data, with two main goals :

- to qualify different available codes by reciprocal comparison;
- to get some preliminary indications about the mechanical behaviour of the structure.

The present work is an analysis of this benchmark performed by means of the structural code ABAQUS and a comparison of the results with those of the INCA code {1}.

The geometric nonlinearity, neglected in {1}, has also been taken into account and its effects underlined.

2) Benchmark

The geometry of the problem is shown in Fig.2 : 1/12 of the cross section of an hexagonal pipe is discretized by 3 x 15 quadrilateral isoparametric parabolic elements.

The loads are :

-a non-uniform temperature distribution across the section;

-a pressure applied on the inner face.

The temperature distribution is given by a thermal analysis of the structure with DELFINE in the conditions specified by a previous thermal benchmark {2}.

The pressure load varies with time according to Fig.1.

The material properties are :

-Young's modulus (GPa) : $E = 194 - 0.0814 * T$ $T < 700$ C
 $E = 277.02 - 0.2 * T$ $T > 700$ C

-Poisson's coefficient : $\nu = 0.3$

-Yield stress (MPa) : $\sigma_e = 702 - 0.545 * T$

-Hardening modulus : (M in Table 1)

-Thermal expansion ($^{\circ}$ C) $^{-1}$: $d = (16750 + 2.76 * T) * 10^{-9}$

-Ultimate yield stress (MPa) : $\sigma_u = 879 - 0.628 * T$

-Ultimate yield strain : $\epsilon_u = \exp\{-5.36 + 933/(T + 273)\}$
(plastic) + $\exp\{7.87 - 15559/(T + 273)\}$

Beside the benchmark assumes the following hypothesis :

-plane strain

-Von Mises yield criteria

-isotropic hardening

TABLE 1
Material properties

T	E	σ_e	M	α
(°C)	(GPa)	(MPa)	(MPa)	(10^6°C) ⁻¹
400	161.44	484.0	7301	17.85
500	153.30	429.5	8160	18.13
600	145.16	375.0	8706	18.41
700	137.02	320.5	8855	18.68
800	117.02	266.0	8207	18.96
900	97.02	211.5	6394	19.23
1000	77.02	157.0	3941	19.51
1100	57.02	102.5	2037	19.79
1200	37.02	48.0	986	20.06
1300	17.02	0	477	20.34
≥ 1385 (*)	0	0	0	20.57

(*) : Melting temperature

3) Calculations

Two main ABAQUS calculations have been performed :

- 1) ABAQUS-P : geometrically linear model
- 2) ABAQUS-G : geometrically non linear model

Both use plane strain elements (eight nodes , reduced integration) with automatic time step control between assigned maximum and minimum values (0.01-1.00).

In Fig.3 is shown the behaviour of the time step as the calculation proceeds.

We remark that the time step has been reduced by the automatic control only in the final part (the reduction at 21s is due only to a problem of the code with the input data).

The two calculations have been stopped respectively at 25.4s and 27.5 s for time step (required for convergence) below the allowed limit.

The material properties assumed for ABAQUS near and above melting temperature are given in Table 3 , while in Table 2 we recall the restrictive hypothesis we had to formulate with INCA in order to reach the convergence {1}.

TABLE 2
INCA assumptions

T	E	σ_e	M	α
(°C)	(GPa)	(MPa)	(MPa)	(10^6°C) ⁻¹
≥ 1250	27.02	24.5	731.5	20.20

TABLE 3
ABAQUS assumptions

T	E	σ_e	M	α
(°C)	(GPa)	(MPa)	(MPa)	(10^6°C) ⁻¹
1300	17.02	1.0	426	20.34
1350	7.02	1.0	157	20.48
≥ 1385	7.02	1.0	36	20.57

4) Results

The output required by the benchmark problem are displacements and equivalent stresses and strains vs. time (Fig.4-11) in the center and in the corner of the cross-section (point A through D of Fig.2).

In addition time history plots of the critical strain ratio (defined as the ratio of the equivalent strain to the ultimate yield strain in a material point) are given for the same positions in Fig.12-15.

For the sake of a qualitative comparison in each figure the results of the two ABAQUS calculations (geometrically linear and non linear) have been plotted together with those of a previous INCA calculation (geometrically linear {1}).

It must be remarked anyway that INCA and ABAQUS values do not actually correspond to the same physical position : the former gives the value at the node while the latter in the nearest integration point (curves marked with an asterisk in the legend), with the only exception of the displacements.

A few general remarks can be made in comparing the two linear calculations (INCA-P and ABAQUS-P) :

-there is , on the whole, a good agreement between the two results and most part of the differences seems to be due to the slightly different position of the output points;

-the hypothesis on the material properties required by INCA to

overcome its lack of convergence {1} yields as expected a stiffer structure (Fig.4);

-the equivalent plastic strain in B starts growing rapidly earlier in ABAQUS than in INCA (Fig.9);

-ABAQUS can converge at much larger displacements without any problem , the corresponding equilibrium configurations have anyway no physical meaning being completely outside the range of validity of the linear model.

More interesting are the results of the non linear ABAQUS analysis (ABAQUS-G) because this model allows us to simulate correctly the structural deformation even in the large displacement range, up to the point of collapse.

The deformed configurations in the non linear case are shown in Fig.16 : the structure under the internal pressure tends to assume the much more resistant cylindrical shape (what the linear model was not able to foresee) and the collapse is reached through an uniform swelling of this shape starting at 27.1 s (in the linear case the corner did not share this generalized expansion).

From 27.1 s the can is almost perfectly cylindrical (except in the corner) and that allows us to estimate the magnitude of the residual strength of the section by means of a simple model (see Appendix) of an equivalent circular tube defined as follows :

-the outer radius b equal to the radius of the circumscribed

circle;

-the thickness h evaluated from the position of the melting front along AB in the given temperature distribution;

-the yield stress s_b on the outer face of the tube is given by the elastic limit σ_e corresponding to the temperature T_A of the point A of the section.

Eq.(14) of the Appendix can then be applied to calculate the critical internal pressure of this tube at 27s (when $b=104.6\text{mm}$, $h=2.3\text{ mm}$, $T_A = 1104^\circ\text{C}$, $s_b=100\text{ MPa}$) :

$$P_c = 1.3\text{ MPa at } t=27\text{ s}$$

Recalling that the input pressure at 27 s reaches 1.2 MPa, we can conclude that the 'equivalent' tube will not fail before this time.

We can now observe that the ultimate yield stresses in the actual benchmark problem are much higher than the elastic limits due to strain hardening, so the above rough estimation seems to confirm the ABAQUS prediction of a can failure only after 27 s (last convergence of the code at $t=27.5\text{ s}$).

5) Conclusions

ABAQUS results with the geometrically linear model are on the whole in good agreement with the corresponding INCA analysis.

The ABAQUS calculations have been carried out without any of the heavy convergence problems shown by INCA {1}.

The non linear analysis points out that the structure by means of large deformations can resist to the increasing internal pressure up to 1.3 MPa and that the hexagonal section collapses like a swelling circular tube at 27.5 s.

Therefore geometric non linearity of the problem has to be taken into account for reliable solutions up to the point of structural failure.

FIG. 1

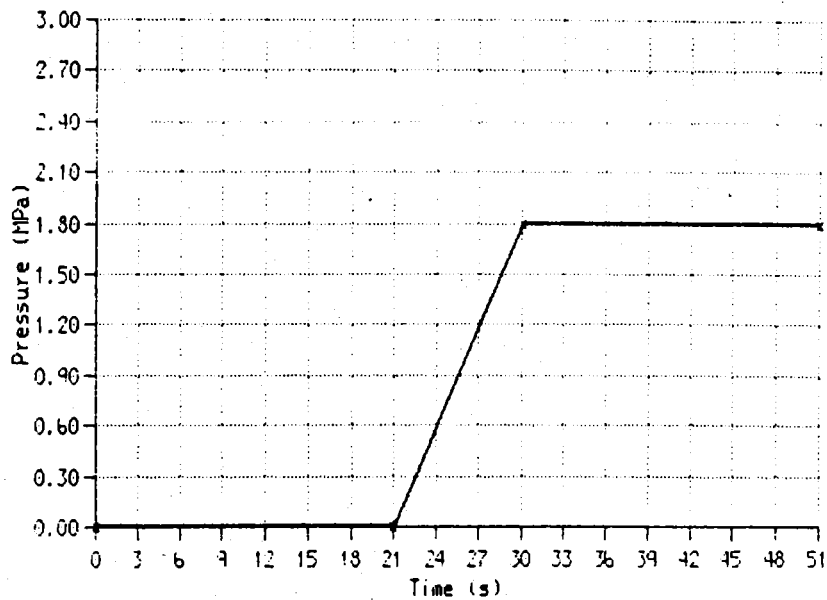


FIG. 2

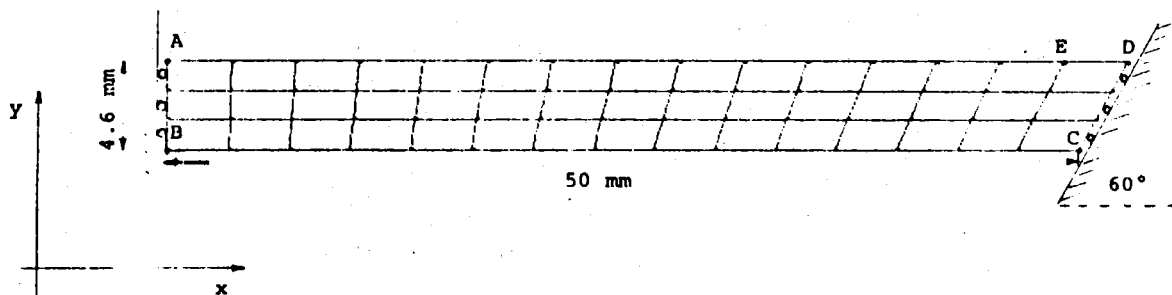


FIG.3 : TIME STEP

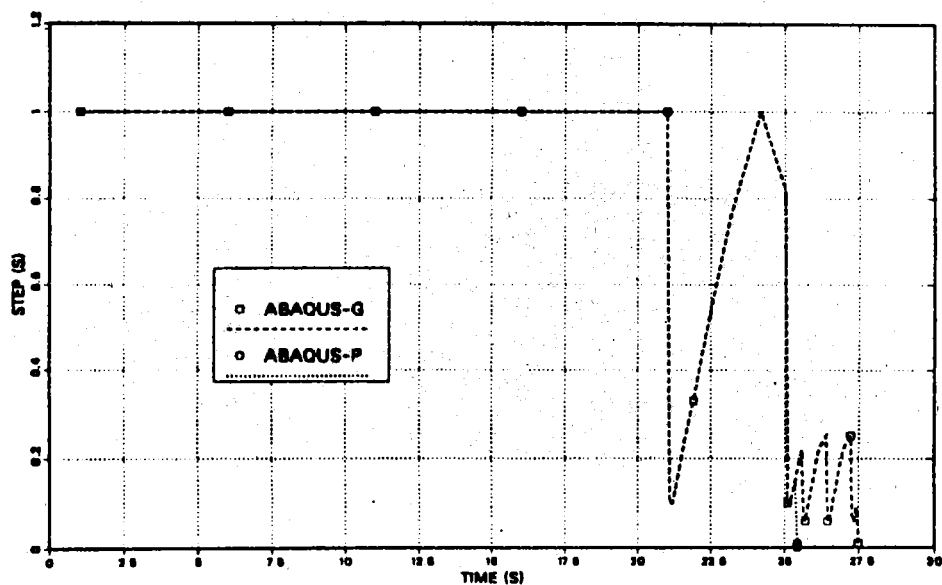


FIG.4 : SPOSTAMENTI IN A

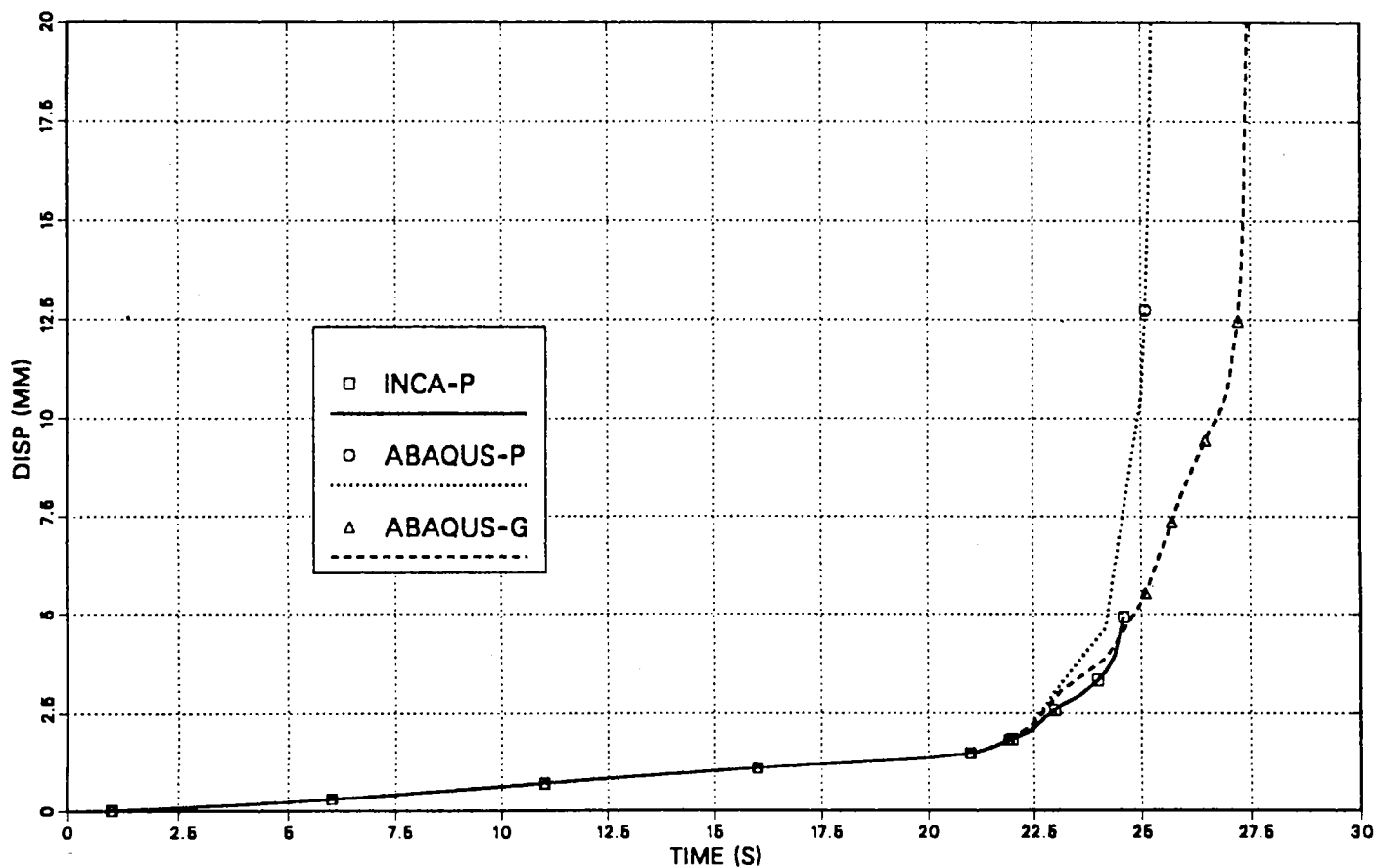


FIG.5 : SPOSTAMENTI IN D

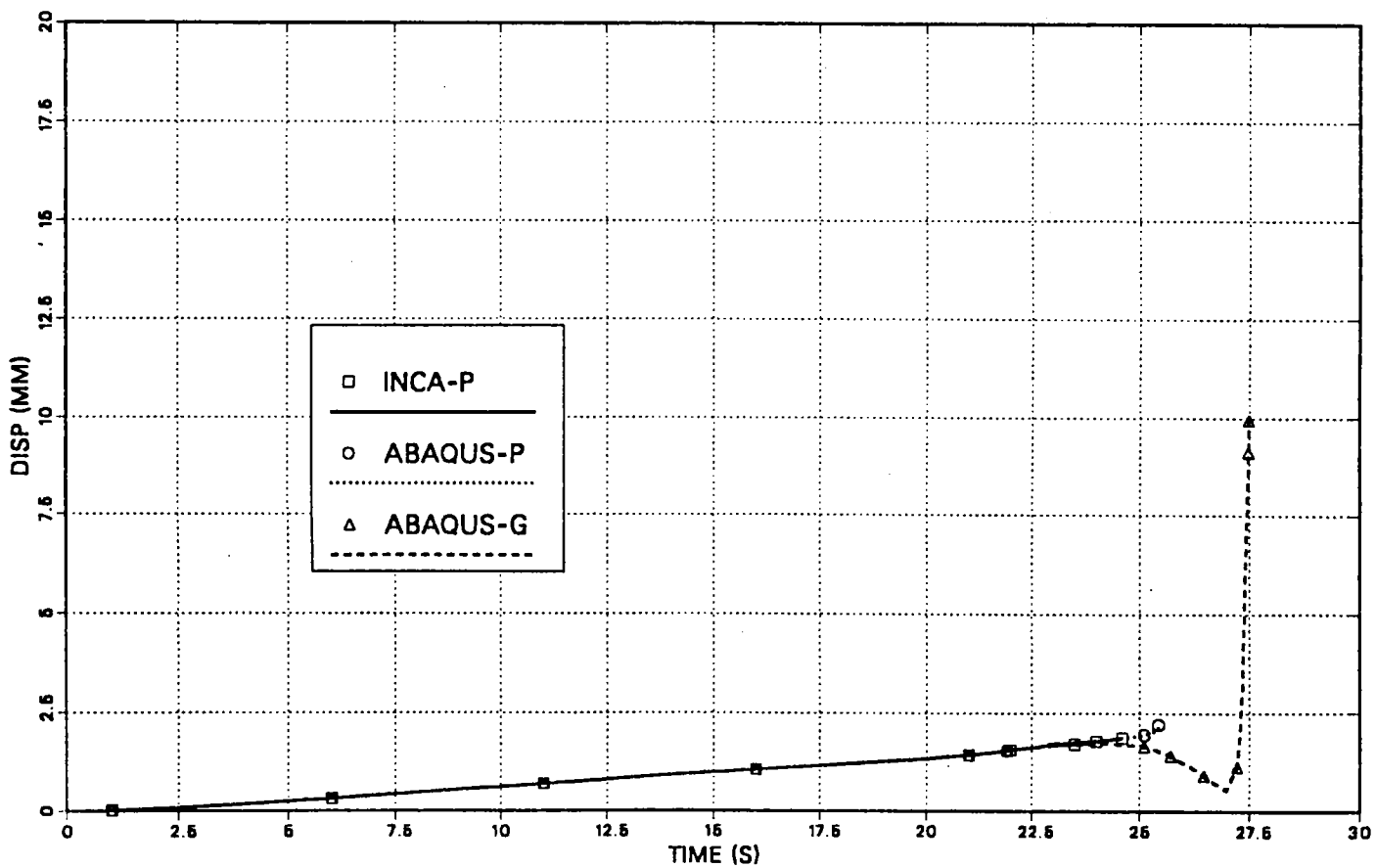


FIG.6 : EQ. STRESS IN A

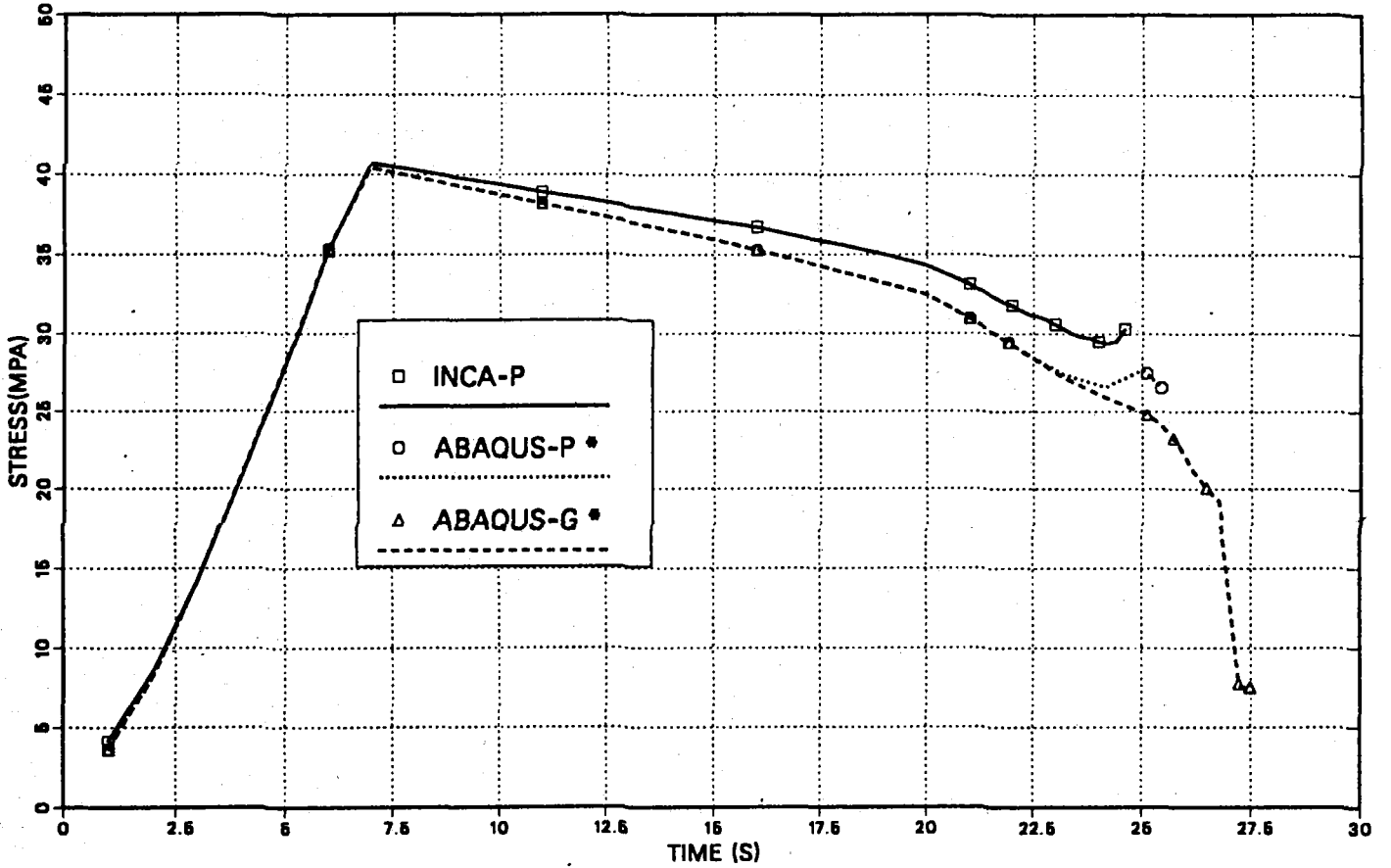


FIG.7 : EQ. STRESS IN B

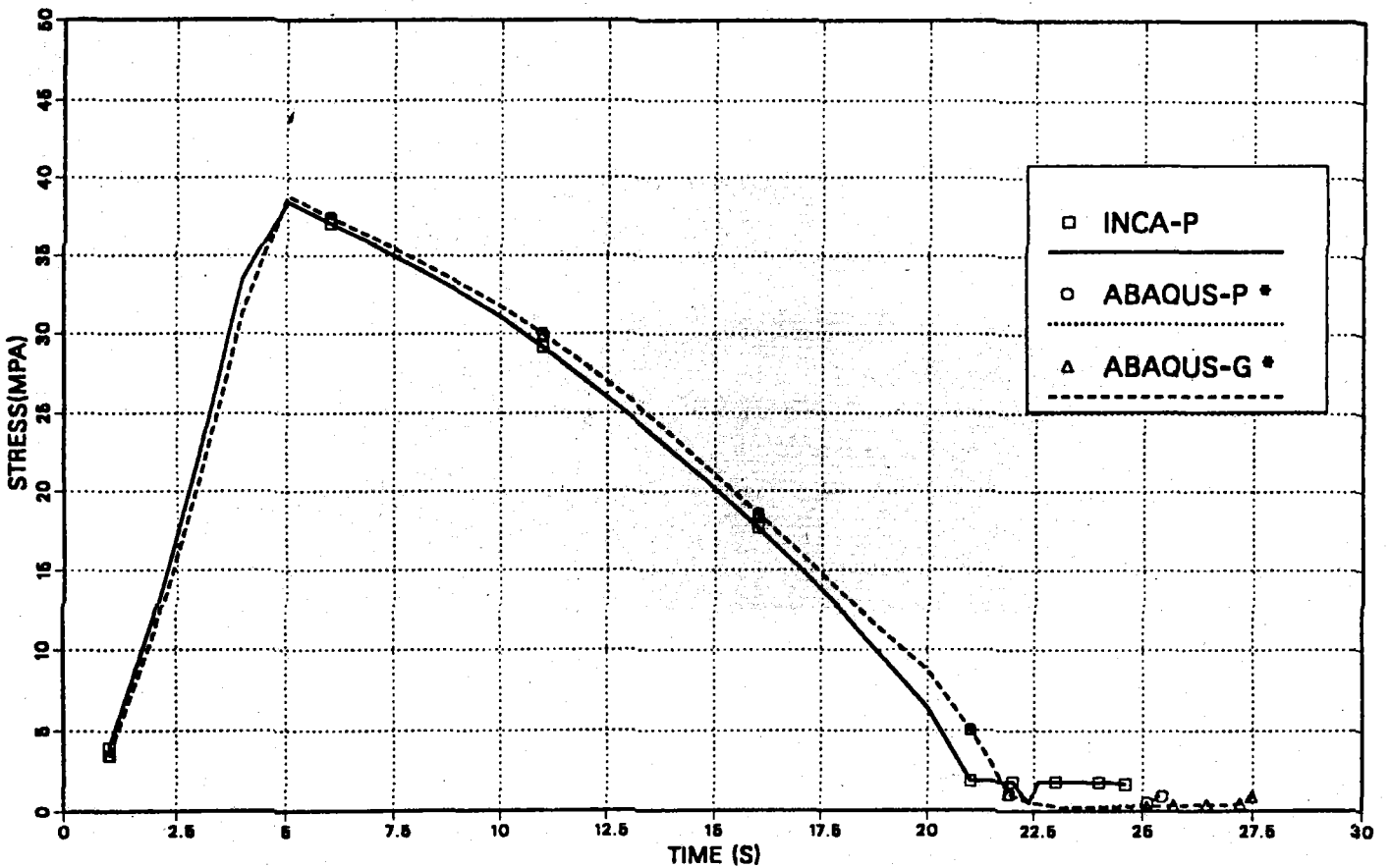


FIG.8 : EQ. STRAIN IN A

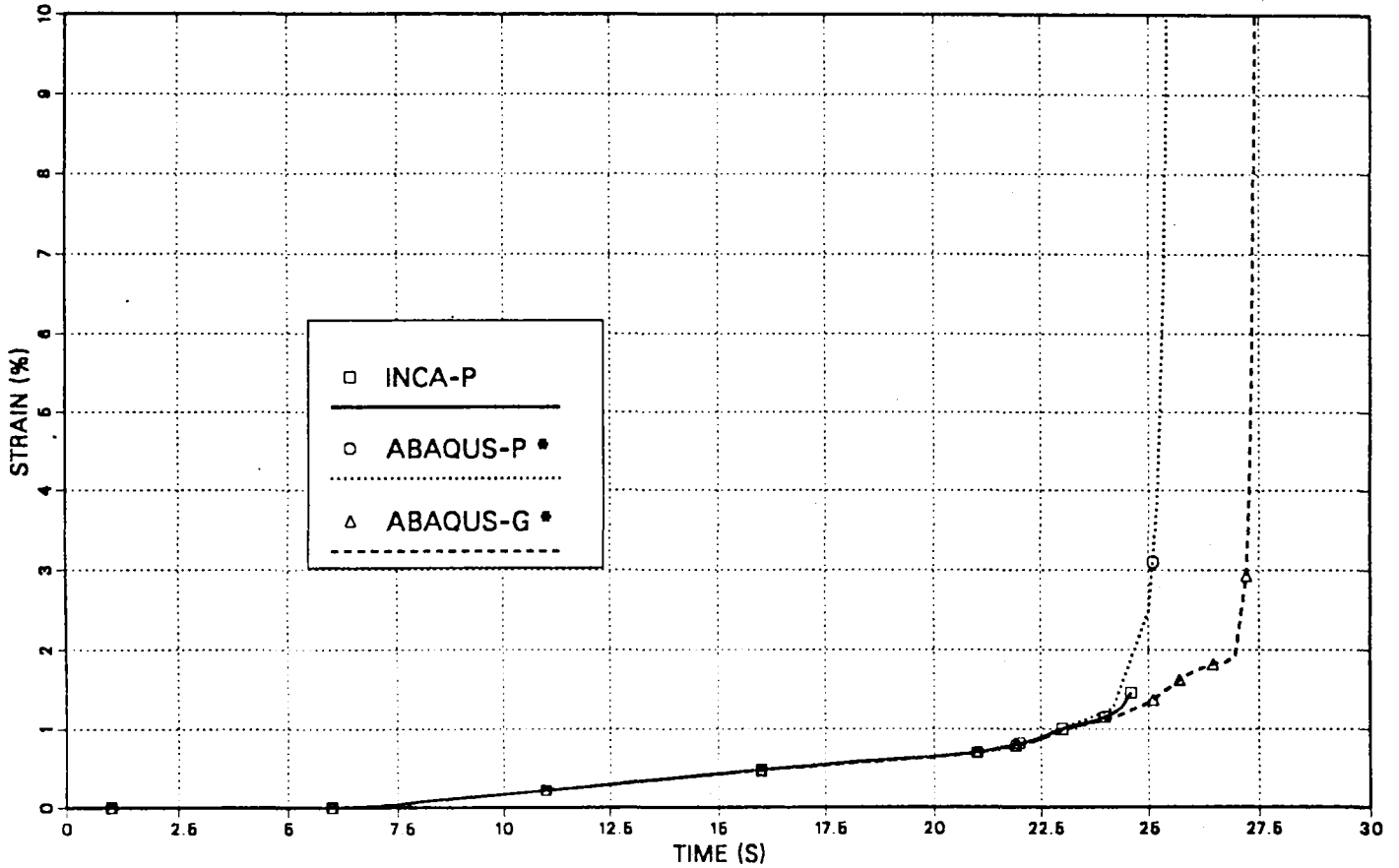


FIG.9 : EQ. STRAIN IN B

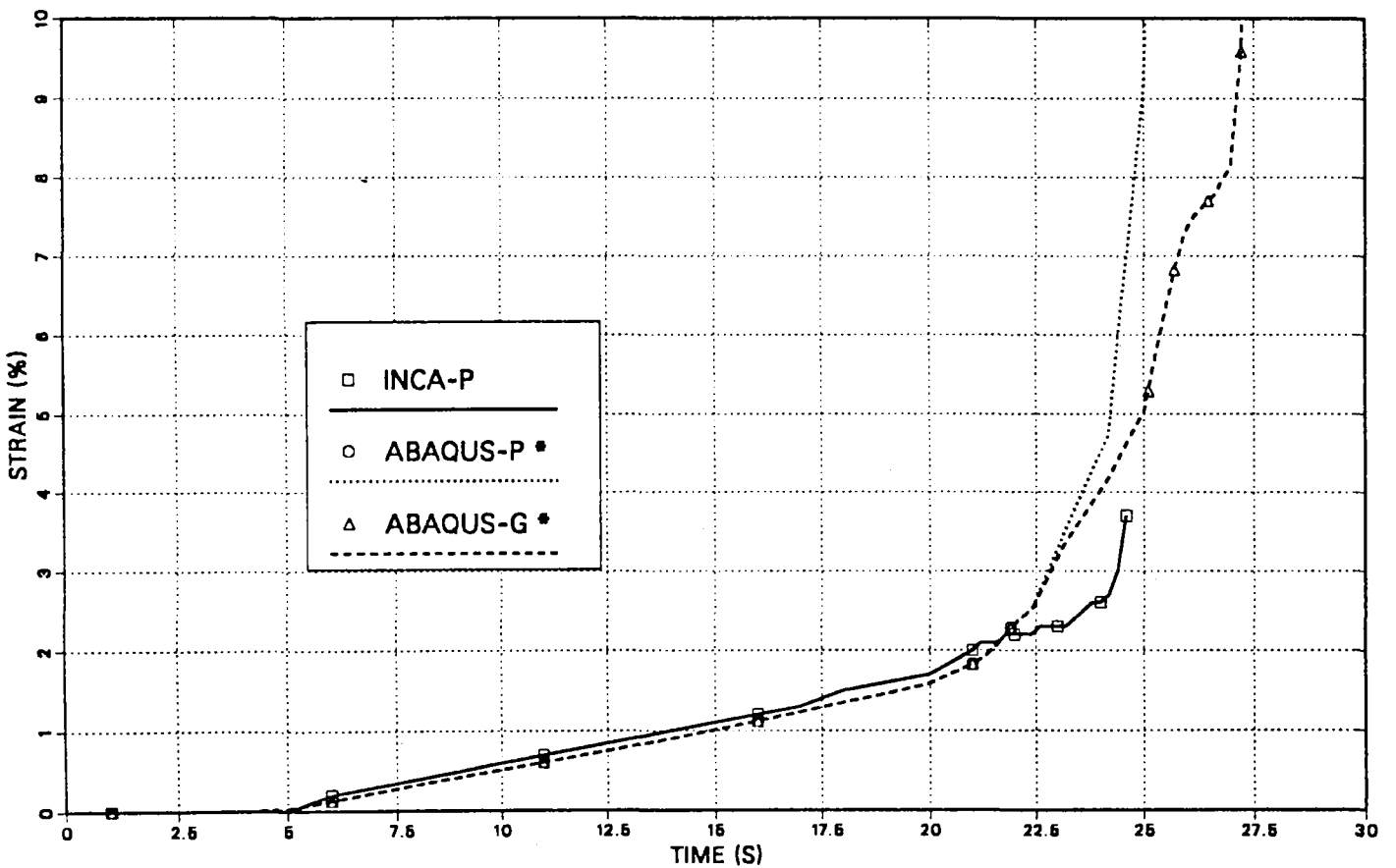


FIG.10 : EQ. STRAIN IN C

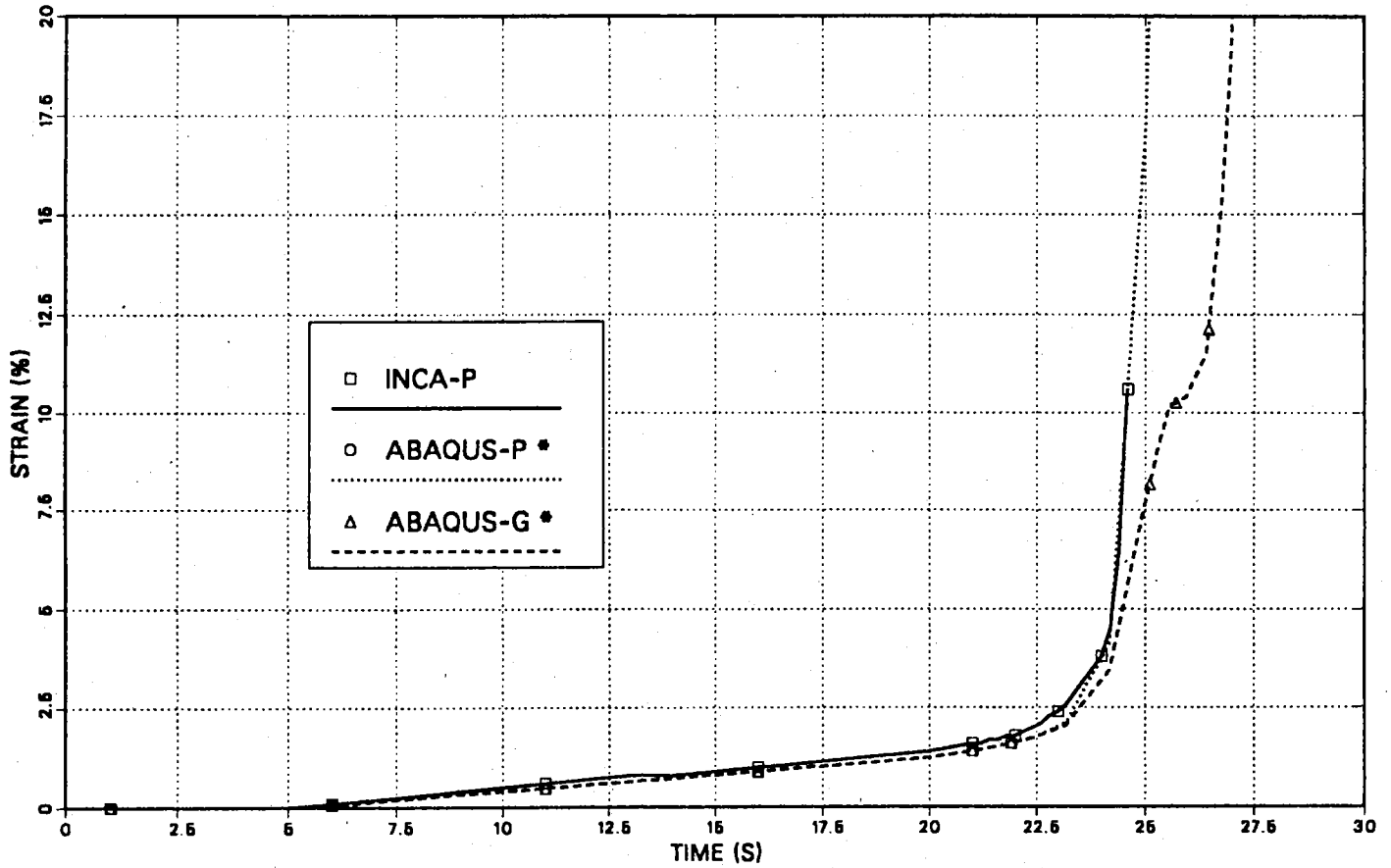


FIG.11 : EQ. STRAIN IN D

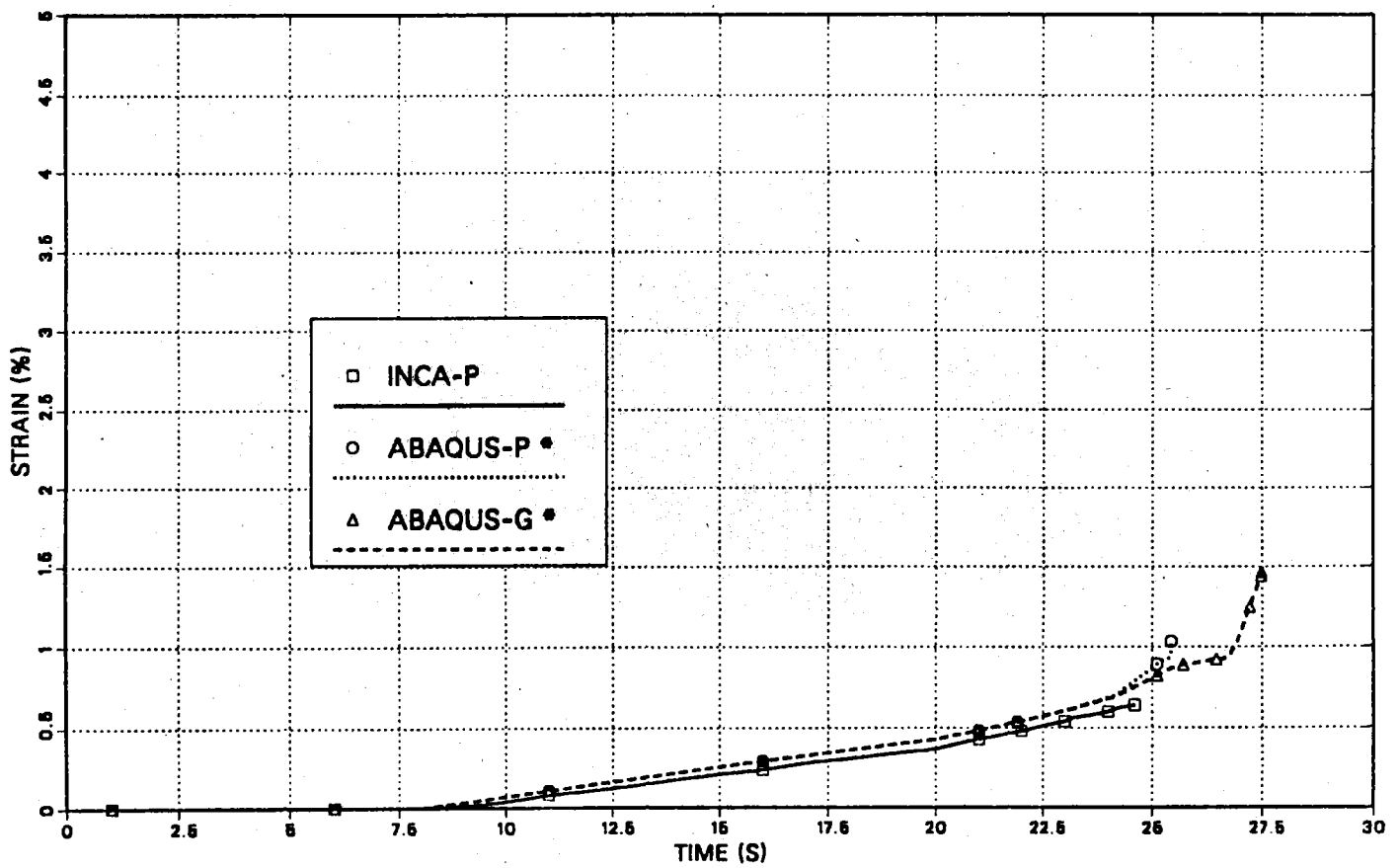


FIG.12 : CRITICAL STRAIN IN A

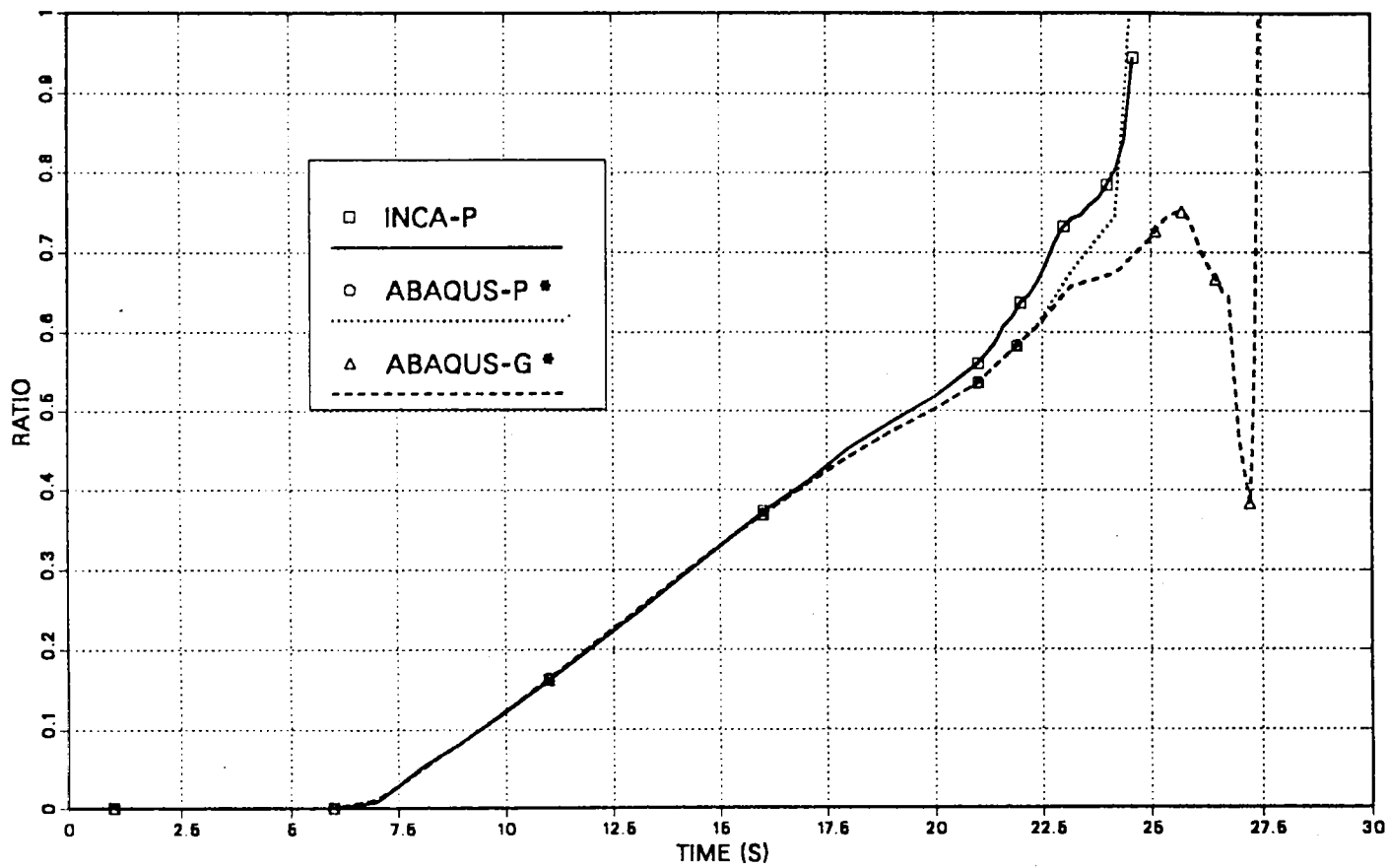


FIG.13 : CRITICAL STRAIN IN B

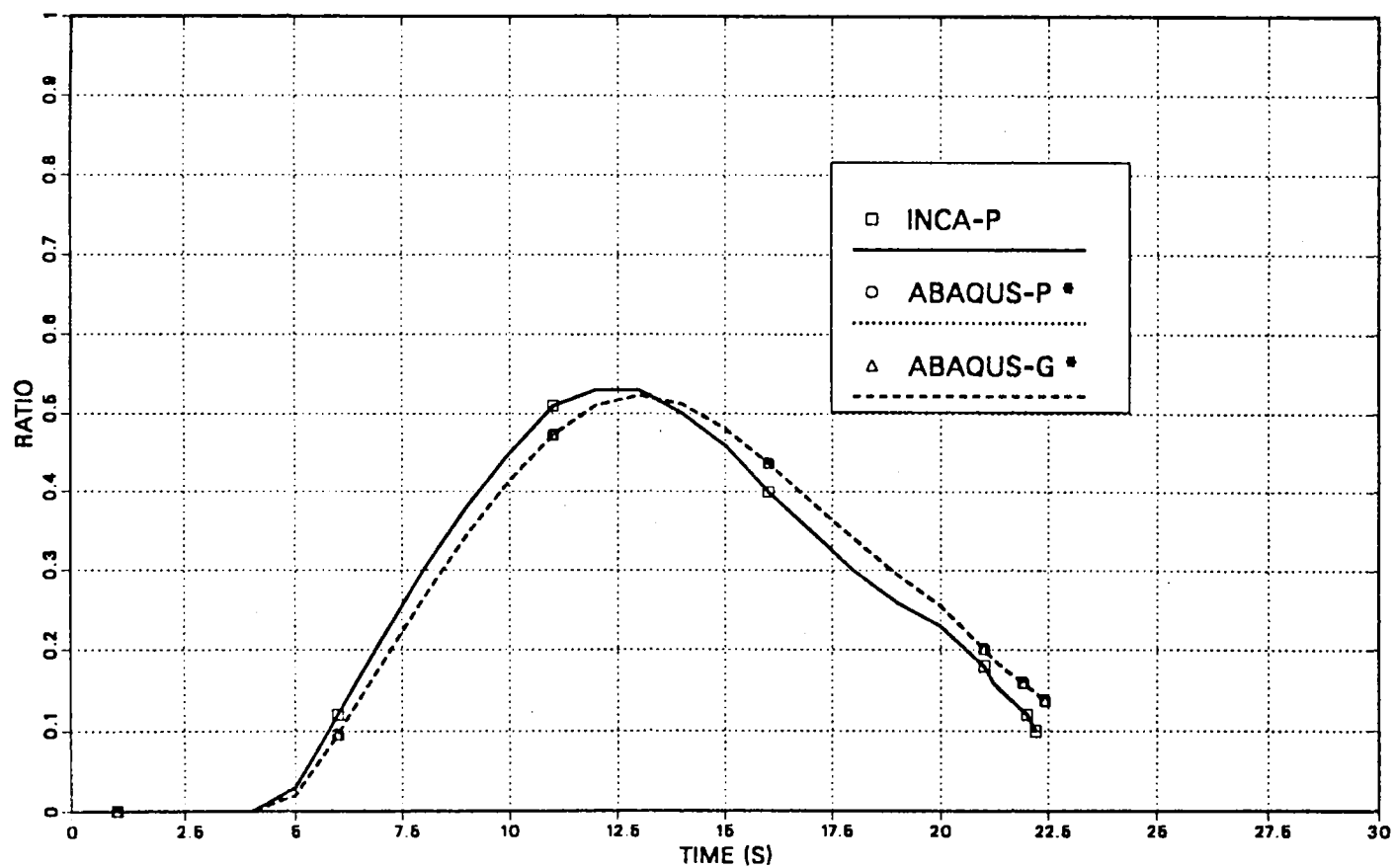


FIG.14 : CRITICAL STRAIN IN C

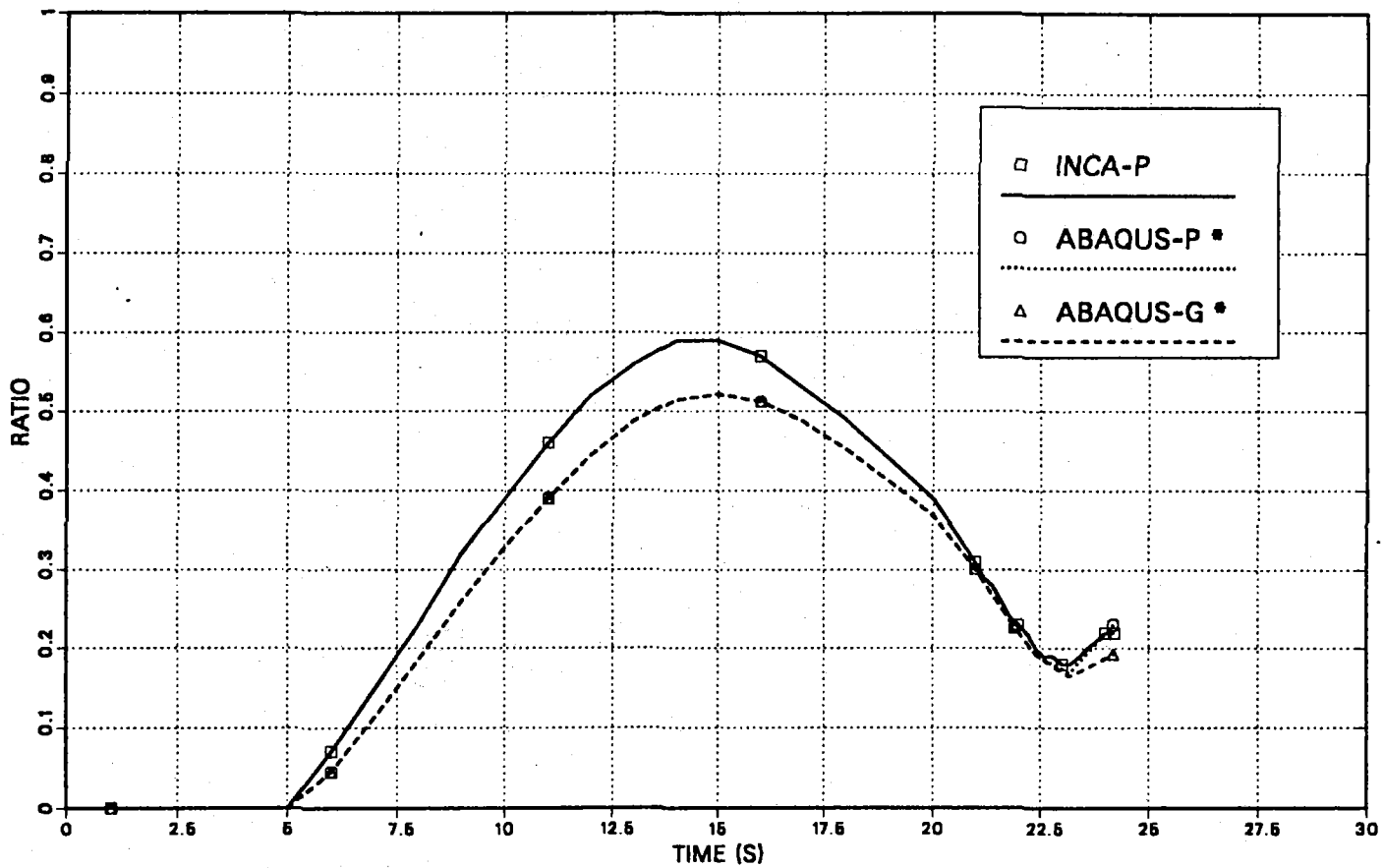


FIG.15 : CRITICAL STRAIN IN D

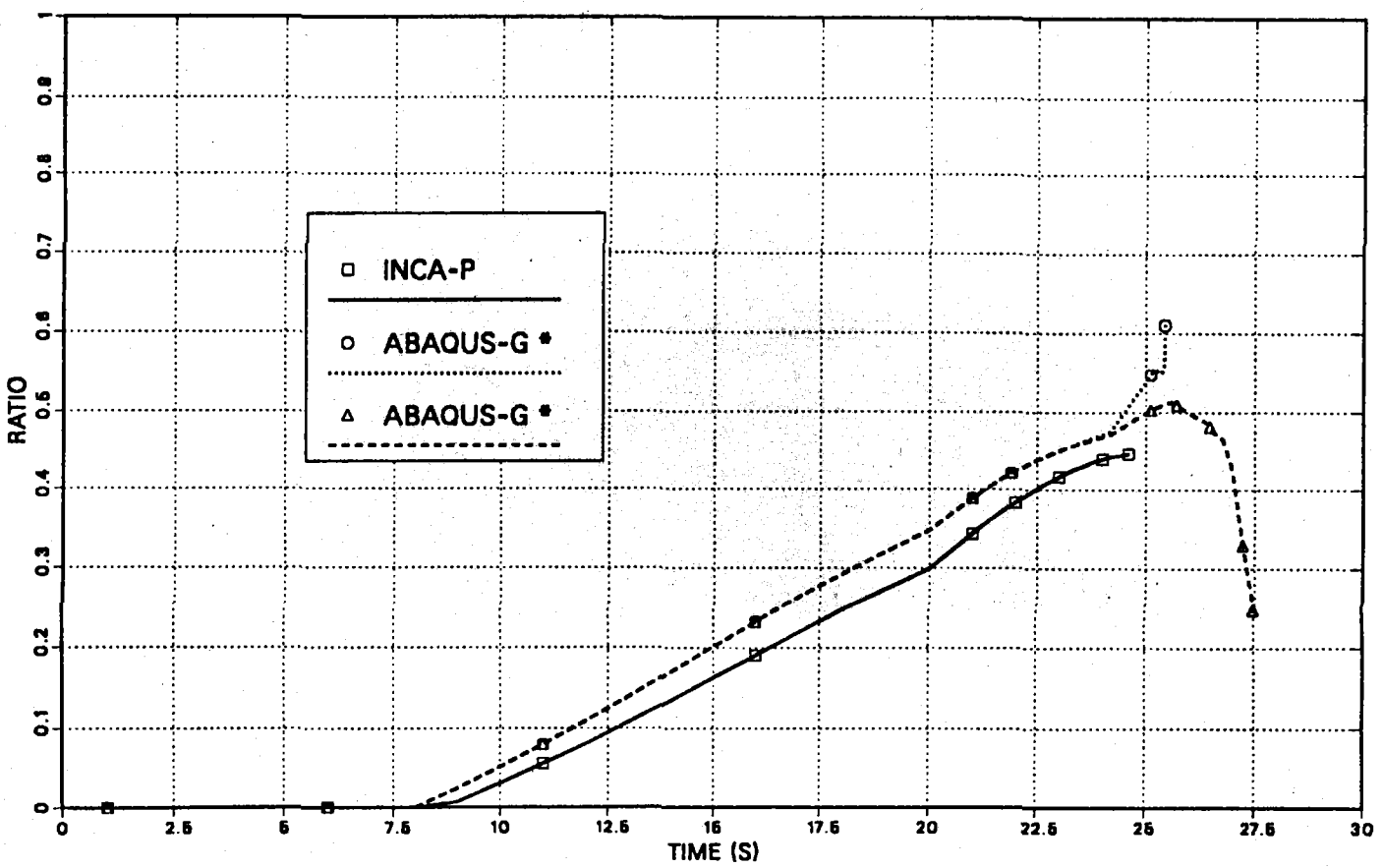
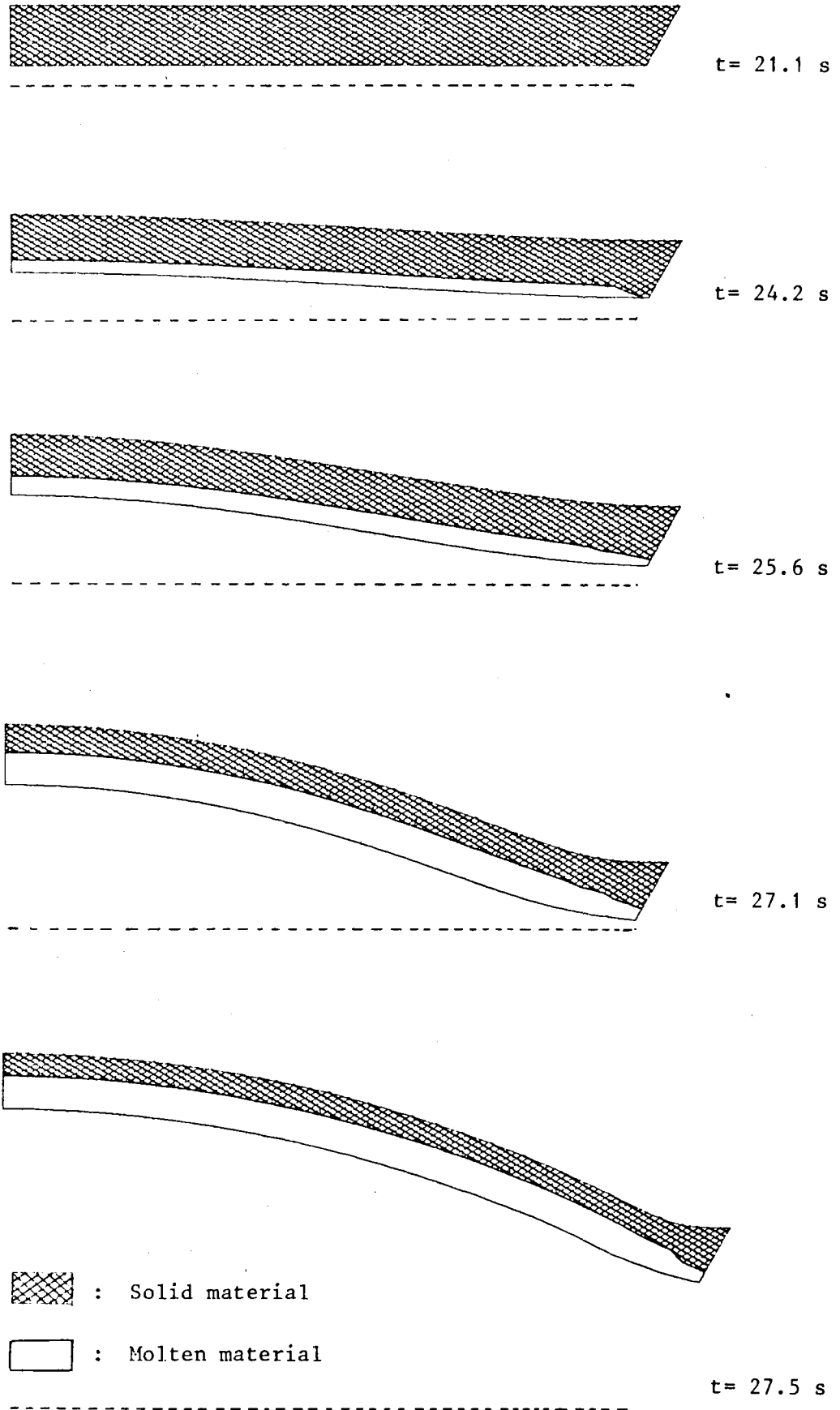


FIG. 16



Appendix

Problem : to find the failure internal pressure of a thick circular tube when the yield stress increases with a given law through the thickness.

For an elastic-perfectly plastic material we can assume as critical pressure the internal pressure which carries to plastic yielding the entire cross-section, because above this value no equilibrium is possible.

The classic solution of this problem for constant yield stress is given for example in {3} and can be easily extended to our case.

If the inner and the outer radius are a and b respectively, the equilibrium equation for the radial direction can be written in the plastic zone as :

$$\frac{ds_r}{dr} - \frac{2*s_y}{\sqrt{3}*r} = 0 \quad (1)$$

where the yield stress s_y is a given function of the radius:

$$s_y = g(r) \quad (2)$$

Integration of the Eq.(1) between a and r , after substitution of Eq.(2) gives :

$$s_r(r) - s_r(a) = \frac{2}{\sqrt{3}} \int_a^r \frac{g(r)}{r} dr \quad (3)$$

For a critical value p_c of the internal pressure this plastic zone will cover the entire cross-section; in that case we can

impose the boundary conditions :

$$\begin{aligned} s_r &= 0 \text{ at } r=b \\ s_r &= -p_c \text{ at } r=a \end{aligned} \quad (4)$$

which allows the determination of the critical pressure p_c .

In fact from Eq.(3) and (4) we get :

$$p_c = \frac{2}{\sqrt{3}} \int_a^b \frac{g(r)}{r} dr \quad (5)$$

This expression can be easily specialized to a linear variation of the yield stress through the thickness :

$$s_y = g(r) = s_a + k*(r-a) \quad (6)$$

where

$$k = \frac{s_b - s_a}{b-a} \quad (7)$$

with s_a , s_b the yield stresses respectively on the inner and outer surface.

In this particular case :

$$p_c = \frac{2}{\sqrt{3}} \left\{ (s_a - k*a) * \ln\left(\frac{b}{a}\right) + k*(b-a) \right\} \quad (8)$$

Introducing $h=b-a$ and Eq.(7) :

$$p_c = \frac{2}{\sqrt{3}} * s_b * \left\{ f + \left(f * \frac{b}{h} - 1 \right) * \ln\left(1 - \frac{h}{b} \right) \right\} \quad (9)$$

where

$$f = 1 - \frac{s_a}{s_b} \quad (10)$$

Finally if the tube is partially molten, we can use Eq.(9) and (10) with $h=h'=b-r_m$, where r_m is the radius of the melting front, and $s_a = 0$ to get :

$$p_c = k * s_b \quad (11)$$

with

$$k = \frac{2}{\sqrt{3}} \left\{ 1 + \left(\frac{b}{h'} - 1 \right) * \ln \left(1 - \frac{h'}{b} \right) \right\} \quad (12)$$

It is interesting to note that for $h, h' \ll b$ Eq.(9) and (11) become respectively :

$$p_c = \frac{s_b * h}{\sqrt{3} * b} * (2 - f) \quad (13)$$

$$p_c = \frac{s_b * h'}{\sqrt{3} * b} \quad (14)$$

References :

- {1} ZUCCHINI, A.,
"A Thermo-mechanical Benchmark Calculation of an
Exagonal Can in the BTI Accident with INCA Code"
NT SYTC/87/1036 , CEA(1987)

- {2} DESPREZ, D.,
Technical Report (to be published), CEA, 1987

- {3} BORG, S.F.,
"Matrix-Tensor Methods in Continuum Mechanics"
D. Van Nostrand Company, Princeton, New Jersey, 1963

**Edito dall'ENEA, Direzione Centrale Relazioni.
Viale Regina Margherita, 125 - Roma
Finito di stampare in ottobre 1988**

**Fotoriproduzione e stampa
a cura della «Arti Grafiche S. Marcello»
Viale Regina Margherita, 176 - Roma**

Questo fascicolo è stato stampato su carta riciclata